Journal of Alloys and Compounds 509 (2011) 9356–9362

Contents lists available at ScienceDirect

Journal of Alloys and Compounds

journal homepage: www.elsevier.com/locate/jallcom

Self-template synthesis of PbS nanodendrites and its photocatalytic performance

Wenqing Wu [a], Yiming He [b], Ying Wu [a,*], Tinghua Wu [a,*]

[a] Key Laboratory of the Ministry of Education for Advanced Catalysis Materials, Zhejiang Key Laboratory for Reactive Chemistry on Solid Surfaces, Institute of Physical Chemistry, Zhejiang Normal University, Jinhua 321004, Zhejiang, China
[b] Department of Materials Physics, Zhejiang Normal University, Jinhua 321004, China

ARTICLE INFO

Article history:
Received 3 November 2010
Received in revised form 13 July 2011
Accepted 13 July 2011
Available online 23 July 2011

Keywords:
Lead sulfide
Nanodendrites
Self-template
Photocatalytic

ABSTRACT

PbS nanodendrites were prepared by a simple hydrothermal process from $Pb(NO_3)_2$ and thiourea (NH_2CSNH_2) at 120 °C without any additives. The structure and morphology of obtained-samples were characterized by X-ray powder diffraction (XRD) and field-emission scanning electron microscopy (SEM). The effect of Pb and S source, the ratio of Pb/S or CTAB/EDA and pH value on the morphologies of the products were investigated. A possible formation mechanism of PbS nanocrystals was discussed based on their shape evolutions. The photocatalytic property of PbS dendrites was also investigated. It was found that the novel nanocrystals have high catalytic efficiency for the degradation of Rhodamine B (RhB) under visible irradiation.

1. Introduction

Lead sulfide (PbS), as an important IV–VI group semiconductor, has attracted considerable attention owing to its especially small direct band gap (0.41 eV) and a larger excitation Bohr radius of 18 nm. It has been widely used in many fields such as Pb ion-selective sensor, photography, IR detector, optical switch and solar absorber [1–5].

Because the morphologies have some influence on the properties, these years PbS nanocrystals with various morphologies, including dendrites, star-shaped, nanoclusters, nanowires, nanorods and flower-like structures, have been prepared [6–9]. Ding et al. synthesized PbS nanowires [10], employing $Pb(AC)_2$ and thiourea as reactant and CTAB/SDS as capping agents. PbS nano- and micro-crystals including nanocubes, comb-like dendrites and cross-shaped crystals have been synthesized by Chen and his co-workers through changing the initial pH value of the reaction solution [11]. PbS nanorods, nanobelts, nanovelvet-flowers and dendrites have been synthesized by Li and his co-workers through surfactant-assisted method [12]. Marangoni et al. studied the controlled-synthesis of PbS nano- and micro-crystals, including star shape particles, diamond shape particles, cubes and octahedrons, by chemical bath deposition method, using different surfactants (including N,N′-bis(dimethyldodecyl)-1,6-hexanediammonium dibromide; N,N′-bis(dimethyldodecyl)-1,8-octanediammonium dibromide, etc.) [13]. Among the different morphologies, PbS nanodendrites have been paid much attention for the special geometric configurations and application prospects. Qian and his co-workers used $PbCl_2$, thiourea, triethylene glycol as solvent to synthesize PbS nanodendrites by solvothermal process [14]. Fenske and his co-workers synthesized PbS dendrites using CTAB as template [15], and some organic reagents (such as ethanol [2], triethylene glycol [14], L-lysine [11], ethylenediamine [16], ethylene glycol [17] and so on) as the solvent system. Although PbS dendrites could be synthesized by different method, the templates or organic reagents had to be used during the synthesis process, which is high cost route and makes against environment. To the best of our knowledge, the synthesis of PbS dendrites by self-template or without any organic reagents have not been reported to date.

In this work, we present a simple, low cost, environment-friendly, self-template hydrothermal method to synthesize PbS nanodendrites and investigate the effect of some reaction conditions (such as Pb or S sources, the ratio of Pb/S or CTAB/EDA, pH value and so on) on the morphology of PbS. A reasonable mechanism is proposed, which might help to further understand the shape-guiding processes of a wide range of novel PbS crystals.

2. Experimental

2.1. Preparation of PbS nanodendrites

All of the reactants were analytical grade and used without any further purification. In a typical procedure, 0.025 mol (8.31 g) of lead nitrate and 0.025 mol (1.91 g) of thiourea were dissolved into 30 mL deionized water, respectively and mixed under magnetic stirring at room temperature (25 °C). Then the mixture was

* Corresponding authors. Tel.: +86 0579 82283907; fax: +86 0579 82282595.
E-mail addresses: yingwu@zjnu.cn (Y. Wu), thwu@zjnu.cn (T. Wu).

0925-8388/$ – see front matter © 2011 Elsevier B.V. All rights reserved.
doi:10.1016/j.jallcom.2011.07.036

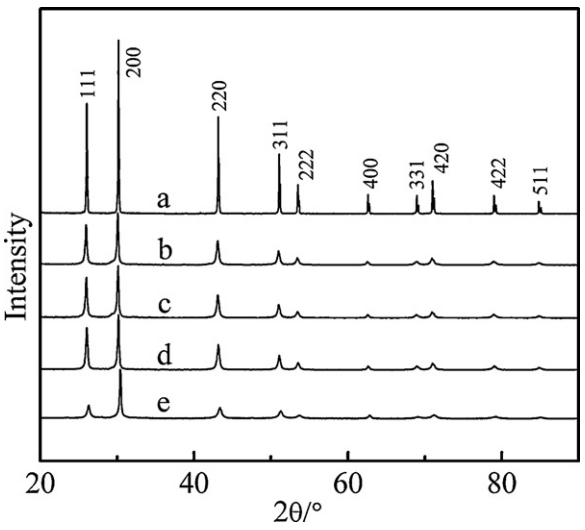

Fig. 1. XRD patterns of the as-synthesized PbS samples with different morphology. (a) Nanoparticle, (b) dentrite, (c) nanoplate, (d) nanorod, and (e) nanoflower.

poured into a 100 mL Teflon-lined stainless-steel autoclave and filled with deionized water up to 70 mL. The autoclave was sealed and aged at 120 °C overnight and then cooled to room temperature naturally. The black products were filtered and washed with distilled water and absolute ethanol. After drying in a vacuum at 80 °C for 3 h, the final products were collected for characterization. To investigate the effect of reaction parameters on the morphologies of PbS nanocrystals, a series of experiments were carried out through changing the source of Pb ($Pb(CH_3COO)_2$, $2PbCO_3{\cdot}Pb(OH)_2$–CH_3COOH, $PbSO_4$–CH_3COONH_4) or S (Na_2S, $Na_2S_2O_3$), pH value of reaction environment(pH = 6, 8, 10, 12) and the ratio of Pb/S (1:1.5, 1:1, 1.5:1) or CTAB/EDA (1:1, 5:3, 3:5).

2.2. Characterization of prepared samples

The as-prepared powder samples were characterized by X-ray powder diffraction (XRD) on a Philips X-ray diffractometer (PW3040/60) using Cu Kα radiation at a scan rate of 0.088°/s. The accelerating voltage and current were 40 kV and 40 mA, respectively. The morphologies of the products were examined by a Hitachi S-4800 scanning electron microscope (SEM). The compositions of the samples were analyzed by energy dispersive X-ray detector (EDS, Hitachi S-4800). The laser Raman spectra were acquired on a RM1000 spectrometer made by Renishaw. The laser wavelength was 514 nm (He–Ne laser 3.0 mW). The FT-IR spectra of samples were recorded on a FT-IR spectrometer (Nicolet Nexus 670) with a resolution of 4 cm^{-1}.

2.3. Photocatalytic activity measurements

The photocatalytic properties of PbS nanodendrites were also investigated, and the general procedure was carried out as follows: a 500 W xenon long arc lamp was used as radiation source. The photocatalytic experiments were carried out in a reactor containing 50 mL of aqueous RhB (5×10^{-6} mol/L) and photocatalysts (50 mg). At first, the suspension was continuously stirred for about 1 h in the dark to ensure an adsorption–desorption equilibrium among the PbS, RhB and deionized water before irradiation. A cutoff filter was used to completely remove any radiation below 380 nm. At given time intervals, the concentration of RhB was monitored by measuring its peak absorbance at 554 nm.

3. Results and discussion

3.1. XRD studies

The phase composition and structure of as-obtained PbS samples with different morphology were examined by XRD. As shown in Fig. 1, all peaks can be readily indexed as face-centered-cubic PbS structure with a lattice constant $a = 5.934$ Å, in agreement with the literature value (JCPDS card no. 5-592, $a = 5.936$ Å) except for the peak intensities, especially for (2 0 0) to (1 1 1). The strong peaks show that the material has good crystallization. No obvious impurity phase was found.

3.2. Effect of Pb/S ratio

To investigate the effect of Pb/S ratio on the morphology of PbS, we synthesized PbS using different Pb/S ratio. When the proportion of Pb to S was 1:1.5 (mole rate), the images of PbS are mainly four-pointed star like and each pointed is consist of tower structured like (Fig. 2a). A typical SEM image of PbS with the ratio of Pb to S of 1:1 clearly shows its dendrites three-dimensions (3D) structures (Fig. 2b). It was interestingly found that four dendrites were composed starfish-like crystals in a certain angle. The individual PbS dendrites have 3D structures with one trunk and four branches,

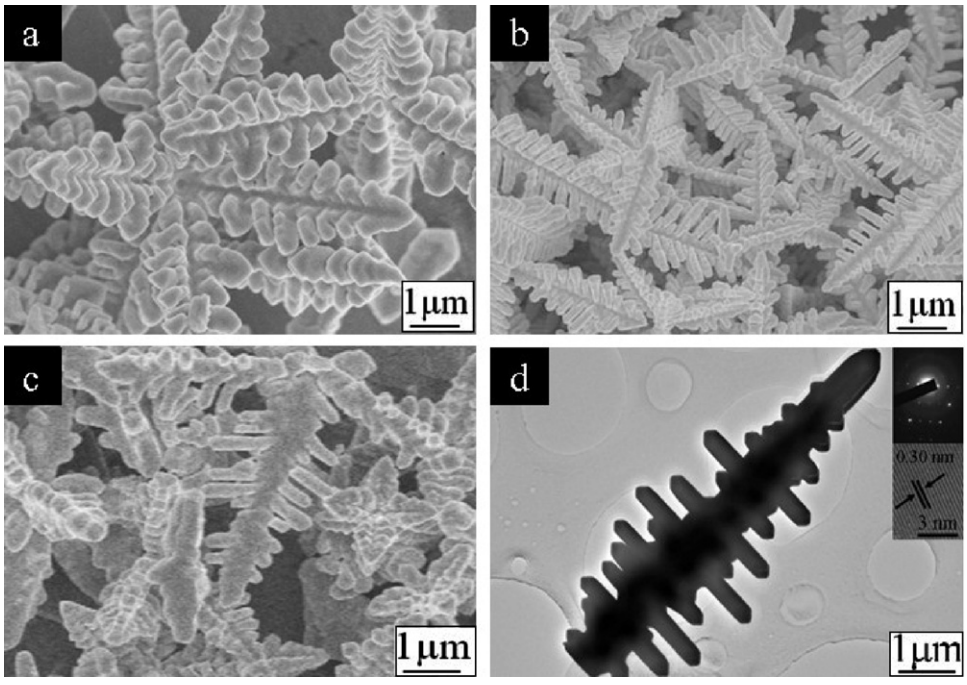

Fig. 2. SEM and TEM images of PbS with different Pb/S ratio. (a) 1:1.5, (b) 1:1, (c) 1.5:1, and (d) TEM image of PbS with Pb/S ratio 1:1, (insert-up) SAED pattern, (insert-down) HRTEM pattern.

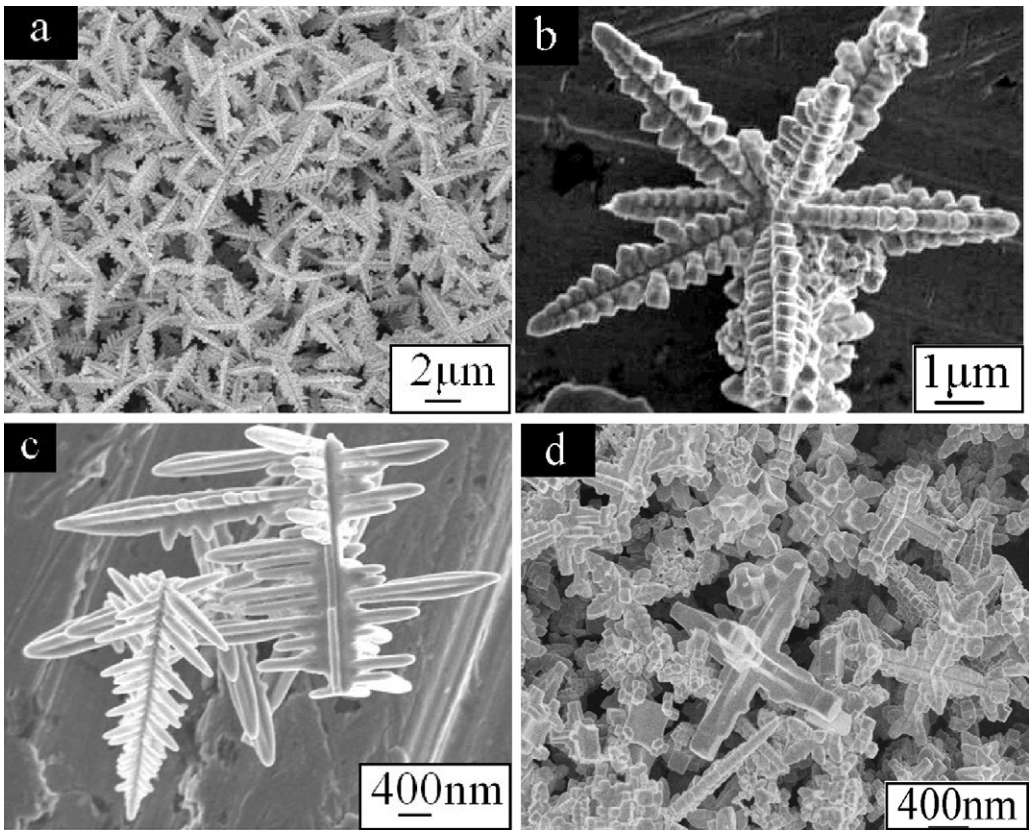

Fig. 3. SEM images of PbS synthesized by different Pb sources (thiourea as the S source). (a) $Pb(NO_3)_2$, (b) $Pb(CH_3COO)_2$, (c) $2PbCO_3{\cdot}Pb(OH)_2$–CH_3COOH, and (d) $PbSO_4$–CH_3COONH_4.

and the nanorods in each branch are parallel to each other and in the same plane. A typical high-resolution transmission electron microscopy (HRTEM) image recorded is shown in Fig. 2d (insert-down), the fringe spacing is determined to be about 0.30 nm, which is close to the (2 0 0) lattice spacing of PbS, indicating that the crystal growth is preferentially in the [1 0 0] direction. From the electron diffraction (ED) patterns (Fig. 2d, insert-up), it can be concluded that the individual PbS dendrite is a single crystal. When the proportion of Pb and S was 1.5:1, both the dendrites 3D structures and octahedral structure can be found (Fig. 2c). It is obvious that the proportion of Pb and S has an effect on the morphologies of PbS, but have no effect on its dimensions. From a kinetic point of view, high supersaturation causes the three-dimensional growth of preformed nuclei and results in the formation of dendrite structure, even octahedral structure, while decreasing the supersaturation favors the formation of concave structure and forms thermodynamically favored bulk cubic morphology [17]. In the present case, the trend of transformation is accord with it, although the dimensions have not changed so clearly with Pb/S ratio. When Pb/S ratio is smaller, the morphology tends to be bulk tower other than dentrite or octahedral structure.

3.3. Effect of Pb sources

In order to investigate the effect of Pb source, we choosed four lead salts ($Pb(NO_3)_2$, $Pb(CH_3COO)_2$, $2PbCO_3{\cdot}Pb(OH)_2$–CH_3COOH, $PbSO_4$–CH_3COONH_4) as the lead sources, fixing the thiourea as the S source. As shown in Fig. 3 several different and special geometric morphologies can be obtained. When $Pb(NO_3)_2$ was used as the Pb source, the products exhibit mainly rod-based dendrites and have even size with good dispersion from the SEM observation (Fig. 3a). Using the $Pb(CH_3COO)_2$ as Pb source, the products still show dendrites morphologies (Fig. 3b). In this system, both the primary and the secondary arms of the dendrites exhibit aggregations of PbS nanoparticles with diameters about 40 nm rather than single-crystalline rod-like morphologies, but the secondary arms still show the tendency to form perpendicularly to the primary arms. When $2PbCO_3{\cdot}Pb(OH)_2$–CH_3COOH was used instead of $Pb(NO_3)_2$ or $Pb(CH_3COO)_2$ (Fig. 3c), the products show one typical morphology of PbS, having 3D structures with one trunk and four branches and some nanorods in each branch are parallel to each other and in the same plane. When $PbSO_4$–CH_3COONH_4 was used as the Pb source, the products show various morphologies (Fig. 3d), including some crosses with different dimensions, dendrites and cubes. In a word, although the lead source plays important role in the morphology of PbS, the trend of crystal growth to special geometric configuration has not been changed.

3.4. Effect of S sources

In order to investigate the role of S source, we used Na_2S, $Na_2S_2O_3$ to replace thiourea and the other conditions were not changed. The products images are shown in Fig. 4. Using Na_2S as S source, PbS nanoparticles could be obtained (Fig. 4a), which are dispersed well and the grain diameter about 80 nm. When using $Na_2S_2O_3$ as the S source, the obtained products exhibit nonuniform size with more dimensions micro-cuboids (Fig. 4b). Through the experiment we can find that only PbS with non special geometric configurations can be obtained with the absence of thiourea. These results are in basic agreement with that reported by Fenske et al. [15]. They figured that the main reason is likely to be that the reaction rate of Pb^{2+} and S^{2-} is too fast under this reaction condition. However, according to Fenske's results PbS nanodendrites could not be synthesized in the absence of CTAB surfactant

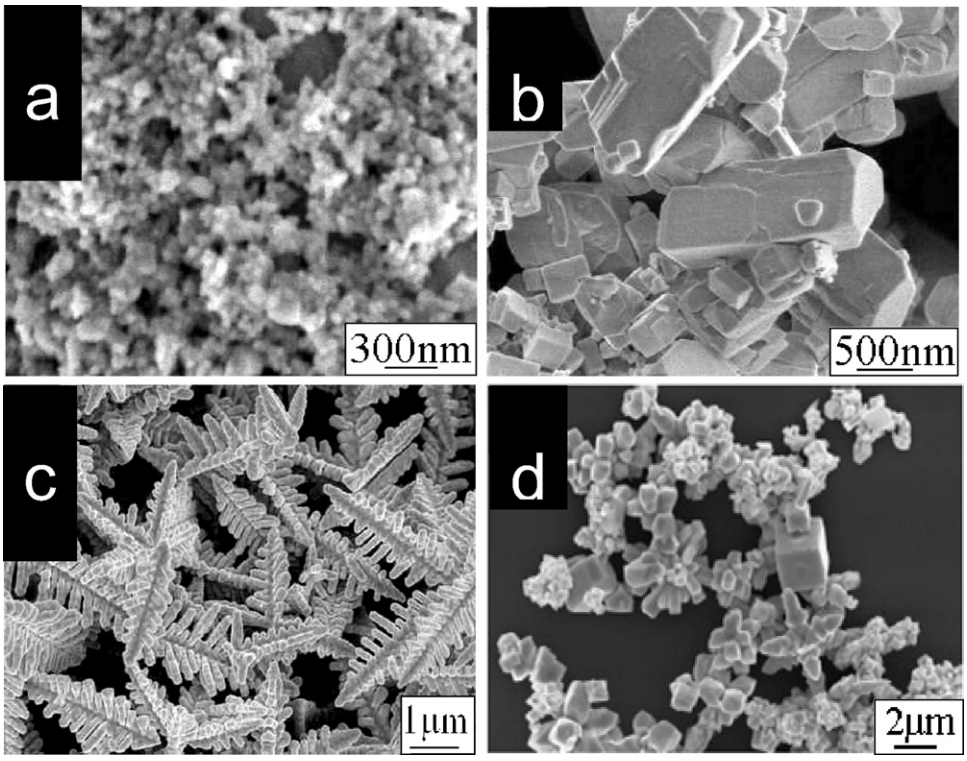

Fig. 4. SEM images of PbS synthesized by different S sources ($Pb(NO_3)_3$ as the Pb source). (a) Na_2S, (b) $Na_2S_2O_3$, (c) $(NH_2)_2CS$, and (d) image from Fenske's paper.

(Fig. 4d), while our experimental results indicate that dendrites (Fig. 4c) can be directly obtained only using $Pb(NO_3)_2$ and thiourea without any surfactant. The main reason may be that in their experiment the concentration of thiourea is too low (0.075 mol/L) to be a self-template agent, while in ours thiourea concentration can reach 0.25 mol/L. So it can be concluded that S source and the concentration of thiourea play the key role to synthesize PbS with special geometric configurations.

3.5. Effect of pH value

In order to further research the generation of PbS, we have regulated the pH value of the reaction environment from 2 to 12 by HCl and $NH_3{\cdot}H_2O$. The results showed that no products could be obtained when the pH value is 2 or 4. Fig. 5b–d images show that nanoparticles can be obtained under alkaline conditions (pH = 8, 10, 12) and the higher alkality the smaller size can be obtained. It is interesting that PbS nanodendrites can be obtained only under the medium acidity conditions. From the experiment results, we can speculate that the hydrolysis rate of thiourea plays the most important role in the generation of PbS with special geometric configurations as the following reaction equations:

$$NH_2CSNH_2 + 2H_2O \rightleftharpoons 2NH_3 + H_2S + CO_2 \quad (a)$$

$$Pb^{2+} + S^{2-} \rightarrow PbS \quad (b)$$

In strong acidic conditions thiourea rapidly decomposes and releases hydrogen sulfide, and lead sulfide cannot be obtained. The ammonia, which is used to be adjusted the basicity, may inhibit the thiourea hydrolysis, and the more concentration of ammonia, the serious inhibition may happen. So the smaller nanoparticles could be gained as the pH value increases. Under the medium acidity conditions, however, thiourea decomposes and releases hydrogen sulfide with appropriate speed and the hydrogen sulfide reacts with Pb ion that have been chelated with thiourea.

3.6. Effect of surfactant

It can be concluded from the quotations mentioned above that the thiourea works not only as S source but also a template agent. To further prove the point we did some experiments as follows. The reaction took place under the same synthetic conditions, except that *N*-cetyl-*N,N,N* trimethyl-ammonium bromide (CTAB) and ethanediamine (EDA) were used as the co-surfactant. The products morphologies are shown in Fig. 6. The flower-like PbS consisting of many nanosheets with thickness of 20 nm was obtained when the ratio of CTAB and EDA is 1:1. Nanorods and nanoplates can be obtained when the CTAB/EDA ratio is 5:3 and 3:5, respectively. As we know, CTAB and EDA are often used as the structure directing agent. In this experiment CTAB/EDA may bond to PbS crystal seed, and so the addition of CTAB/EDA can have some the effect on thiourea, which cause all the main PbS nanodendrites change into different morphologies. According to the results from Dong et al. [12], there exists three factors related to the formation of PbS, including the selective adsorption of surfactant on PbS crystal faces, the slow releasing rate of H_2S on the interface of oil and water, the initial formation of solid basic nitrate of lead. For the reaction system without surfactant, only the last factor controlled the rate of nucleation, so at the same time of the crystal growing along the (1 0 0) axis to form the trunk, it also grew laterally to form the primary branches even the second order branches. The addition and adsorption of surfactants led the PbS crystal to grow directionally along a certain crystal faces. In this reaction system, mixed agents CTAB/EDA were used as "capping reagent" and had cooperating function to bond with solid surface and adsorb on the selective faces of PbS to control crystal growth direction consequently. The equal amount CTBA/EDA can stabilize charged (1 1 1) face rather than the uncharge (1 0 0) face, and accelerate the growth of (1 0 0) faces relative to (1 1 1) face. When the ratio of CTAB/EDA was increased, the (0 1 0) and (1 0 0) faces were selectively adsorbed and thus nanorod was formed. In comparison, when CTBA/EDA was higher, the capping agents were supposed to bond preferentially

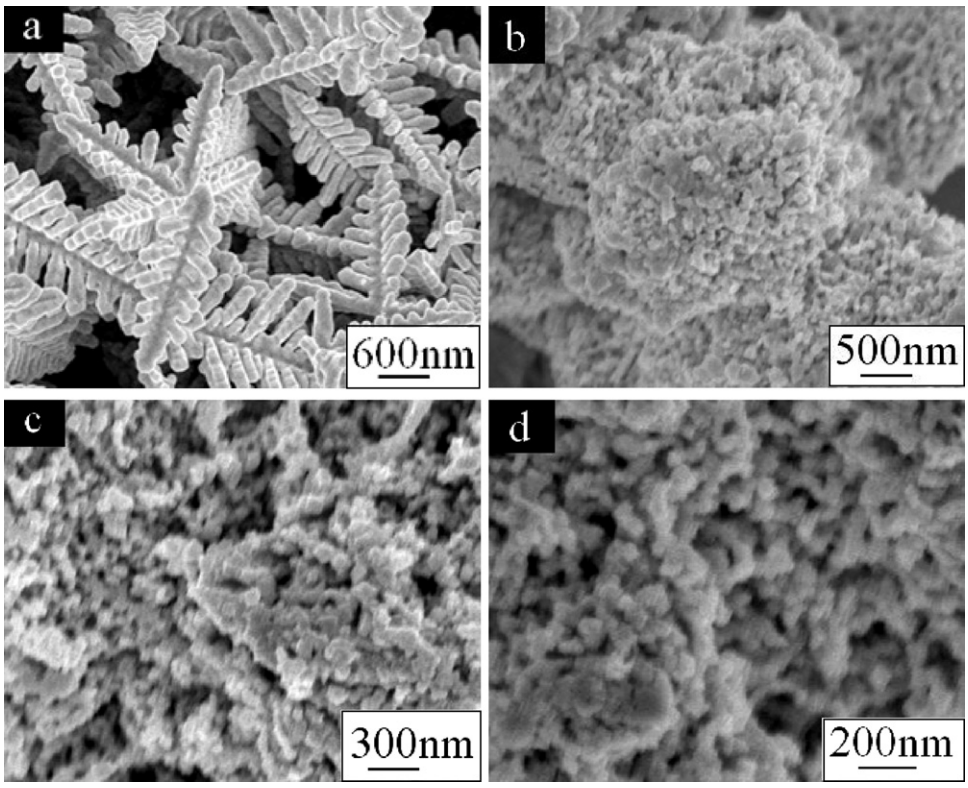

Fig. 5. SEM images of PbS synthesized at different pH value. (a) 6, (b) 8, (c) 10, and (d) 12.

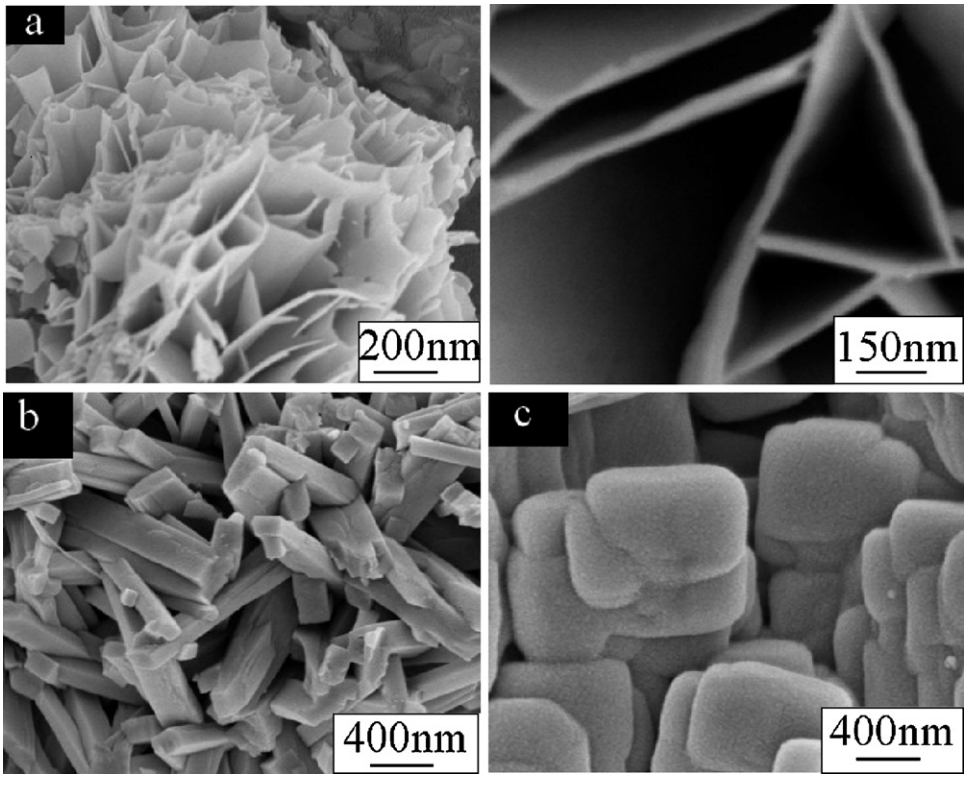

Fig. 6. SEM images of PbS synthesized with different surfactants ratio of CTAB and EDA (in mol rate). (a) 1:1, (b) 5:3, and (c) 3:5.

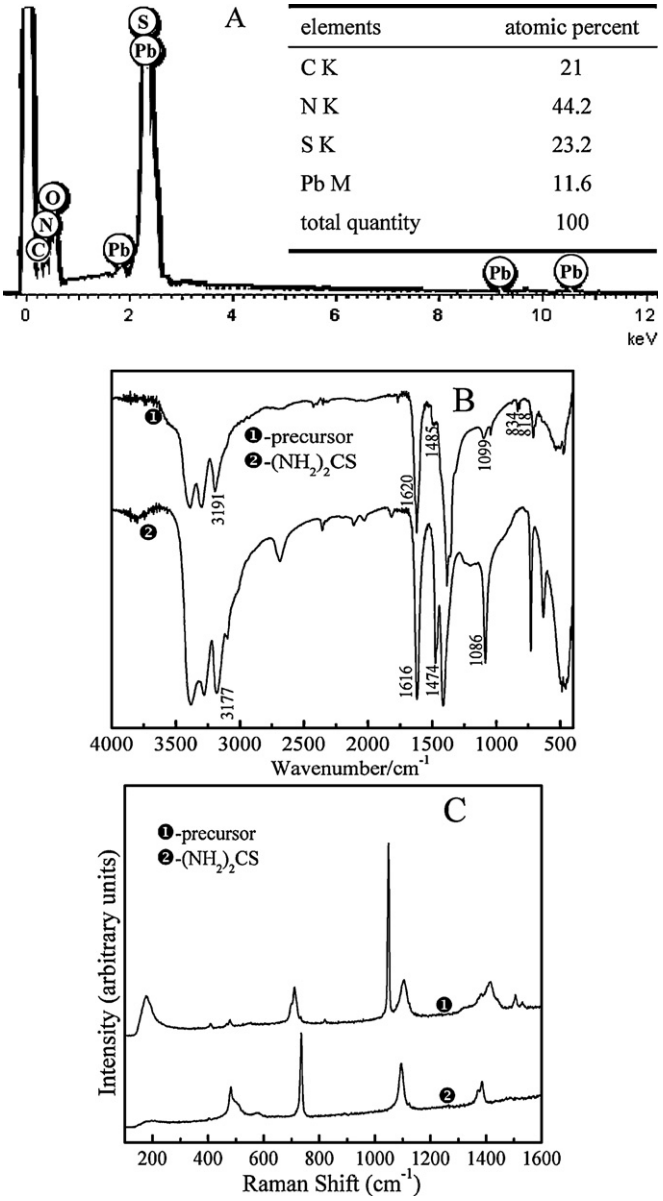

Fig. 7. (A) EDS, (B) FT-IR, and (C) Raman analysis results for the complex precursor.

to the (0 0 1) face, resulting in the formation of lamellar micelle. Of course, the exact mechanism of the morphologies evolution of PbS nanostructure is still not fully understood and further studies are needed to explain the observed phenomena.

3.7. Complex precursor formation and determination

Is PbS produced from the decomposition of a complex of Pb–thiourea or the direct reaction of Pb^{2+} and S^{2-}? To investigate the reaction route, we did elemental analysis, FT-IR measurement, and optical characterization. It is worthy of being mentioned that when $Pb(NO_3)_2$ was dissolved into an early formed white solution of thiourea, the solution color changed from white to greyish white gradually. The changed color of the mixture reveals the formation of a complex precursor in the solution. For determination, the precursor was extracted and purified. The experimental details were as follows. Firstly, 0.025 mol $Pb(NO_3)_2$ was dissolved into a aqueous solution (35 mL) and mixed with 0.025 mol thiourea in 35 mL deionized water, and the solution was stirred for 25 min. Then, the solution naturally formed two phases: an achromatous aqueous phase and a greyish white solid phase. The solution was allowed to stand for another 25 min to ensure complete separation of the two phases, then the greyish white phase was separated, and washed several times with distilled water, dried at 60 °C and a greyish white powder was obtained. Elemental analysis (EDS) (shown in Fig. 7A)of the product deduces a formula of Pb–(thiourea)$_2$ for the complex, since the molar ratio of C:N:S is: 1.9:4:2.1, and a calculated molar ratio of S:Pb is 2:1. To further confirm the structure of the precursor, it was characterized by FT-IR with a pure thiourea for reference. As shown in Fig. 7B, it is found that there are some changes between the as-prepared precursor and the pure thiourea. Obviously, the frequency of the C=S stretching vibration in pure thiourea shifted from 1086 to 1099 cm^{-1} in Pb–(thiourea)$_2$. The increased frequency of the C=S stretching vibration and new weak-absorption band of C–S (834, 814 cm^{-1}) imply that sulfur atom of thiourea coordinate with the metal ion [18]. At the same time, the strong absorption peaks of pure thiourea at 1616 cm^{-1} and 3177 cm^{-1} of N–H bond in H–N–C group are also shifted to 1620 and 3191 cm^{-1} [16]. The shifts can be attributed to the change of bond character of the nitrogen to carbon in N–H_2 group bonding with the metal ion [19]. Meanwhile, the characteristic bands of C–N stretching vibration 1474 cm^{-1} in pure thiourea was shifted to 1485 cm^{-1} in the complex, so it can be speculated that nitrogen atom of thiourea coordinate with the metal ion. Some new absorption bands appeared in fingerprint region (from 400 to 600 cm^{-1}) are identified as the absorption of Pb–S and Pb–N [20]. Fig. 7C is Raman absorption spectra of the complex and thiourea. The spectra give an intensive absorption centered at 150 cm^{-1} and 1050 cm^{-1} in the precursor, which is consistent with that of Pb–(thiourea)$_2$ [21]. From the above studies, the epi- and bulk phase of the complex are homogeneous and consistent with that of Pb–(thiourea)$_2$ in the reaction system. The complex precursor formed in solutions can be formulated as follows

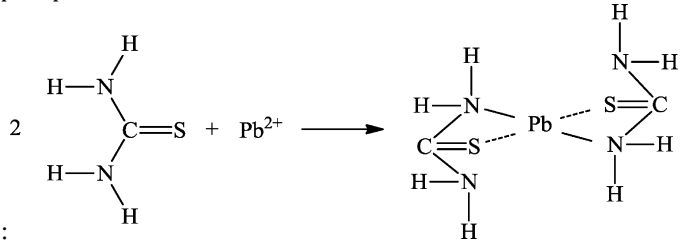

:

Thus we speculated that the formed Pb–thiourea complex served as precursor for the growth of PbS crystals under an elevated solvothermal synthetic route as shown in present experiments.

3.8. Photocatalytic activity of PbS dendrites

In this work, we probed reasonably simple reaction involving the degradation of RhB under visible irradiation conditions in the presence of PbS dendrites. We noted a continual fading of the coloration of RhB with increasing reaction time, in the presence of PbS dendrites or nanoparticles samples, implying a steady, continuous degradation of the organic dyes.

The photocatalytic performance of PbS was estimated by monitoring the intensity of RhB's characteristic absorption at 554 nm as a function of reaction time. The data clearly showed that dendrites and nanoparticles are active photocatalysts, as illustrated in Fig. 8A. Obviously, PbS dendrites exhibited a higher photocatalytic degradation activity compared with the nanoparticles (Fig. 5b) sample. The photocatalytic decolorization reaction of RhB can be modeled as a pseudo-first-order reaction with the kinetics expressed by the equation, $\ln(C_0/C_t) = kt$, where C_0 represents the initial concentration of aqueous RhB, C_t denotes the concentration of RhB at a given reaction time "t", and k is the reaction rate constant[21]. From the linear extrapolations (Fig. 8B), the computed reaction rate con-

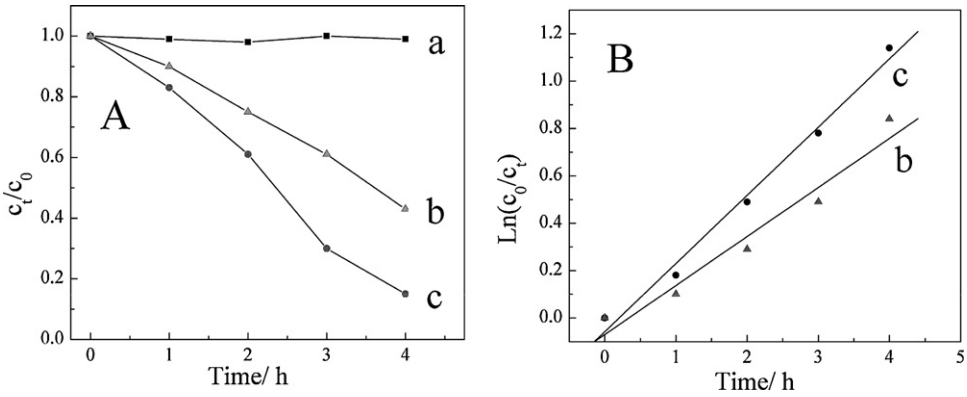

Fig. 8. (A) Photodegradation performance of RhB as a function of reaction time. (B) Plot of the logarithmic change in concentration of RhB as a function of irradiation. (a) A blank control, (b) as-prepared PbS nanoparticles, and (c) as-prepared PbS dendrites.

stants of the PbS dendrites and nanoparticles are $2.07 \times 10^{-1}\,h^{-1}$ and $8.1 \times 10^{-2}\,h^{-1}$, respectively.

The potential photocatalytic mechanism in the degradation of RhB has been previously described and may involve several steps: (1) photoabsorption of the PbS catalysts, (2) generation of photoinduced electrons and holes, (3) transfer of charge carriers to the surface, and (4) recombination of the available charge carriers with reactive, reagent dye molecules [22]. The observed enhancement of photocatalytic activity of as-prepared PbS dendrites herein is most likely correlated with the special geometric configuration as compared with the nanoparticles.

4. Conclusions

In summary, by means of the proper control of the reaction conditions, we have successfully prepared PbS nanodendrites, nanorods, nanoplates, and nanoflowers in aqueous solution at lower temperature. It has been found that all factors of the Pb/S ratio, Pb or S source, pH value and the concentration of thiourea play important roles in the formation of various morphologies of PbS nanocrystals. Especially, thiourea works as not only S source but also template agent in the reaction. The photocatalytic activity test has shown that PbS with special geometric configuration (dendrites) has good photocatalytic activity under visible irradiation.

Acknowledgments

This work is supported by grants from the Nature Science Foundation of China (Nos. 21003109, 21003108) and the Education Department of Zhejiang Province in China (No. Y200909374).

References

[1] L. Xu, W. Zhang, Y. Ding, W. Yu, J. Xing, F. Li, Y.T. Qian, J. Cryst. Growth 273 (2004) 213–219.
[2] A.M. Qin, Y.P. Fang, W.X. Zhao, H.Q. Liu, C.Y. Su, J. Cryst. Growth 283 (2005) 230–241.
[3] S. Wang, A. Pan, H. Yin, Y. He, Y. Lei, Z. Xu, B. Zou, Mater. Lett. 60 (2006) 1242–1246.
[4] Y.C. Zhang, T. Qiao, X.Y. Hu, G.Y. Wang, X. Wu, J. Cryst. Growth 277 (2005) 518–523.
[5] S. Zhou, Y. Feng, L. Zhang, J. Mater. Res. 18 (2003) 1188–1191.
[6] N.L. Heda, A. Rathor, V. Sharma, G. Ahmed, Y. Sharma, B.L. Ahuja, J. Alloys Compd. 463 (2008) 47–54.
[7] S. Jana, S. Goswami, S. Nandy, K.K. Chattopadhyay, J. Alloys Compd. 481 (2009) 806–810.
[8] F. Li, X.T. Huang, T. Kong, X.Q. Liu, Q.H. Qin, Z. Li, J. Alloys Compd. 485 (2009) 554–560.
[9] S. Kaci, A. Keffous, M. Trari, H. Menari, A. Manseri, J. Alloys Compd. 496 (2010) 628–632.
[10] B. Ding, M.M. Shi, F. Chen, R.J. Zhou, M. Deng, M. Wang, H.Z. Chen, J. Cryst. Growth 311 (2009) 1533–1538.
[11] S.F. Shao, G.J. Zhang, H.J. Zhou, P.C. Sun, Z.Y. Yuan, B.H. Li, D.T. Ding, T.H. Chen, Solid State Sci. 9 (2007) 725–731.
[12] L.H. Dong, Y.C.Y. Liu, M.Y. Li, F.Y. Yang, L.L. Li, J. Colloid Interface Sci. 301 (2006) 503–510.
[13] K. Singh, A.A. McLachlan, D.G. Marangoni, Colloids Surf. A: Physicochem. Eng. Aspects 345 (2009) 82–87.
[14] D.B. Wang, D.B. Yu, M.W. Shao, X.M. Liu, W.C. Yu, Y.T. Qian, J. Cryst. Growth 257 (2003) 384–389.
[15] D.B. Kuang, A.W. Xu, Y.P. Fang, H.Q. Liu, C. Frommen, D. Fenske, Adv. Mater. 20 (2003) 15.
[16] W.Q. Zhang, Q. Yang, L.Q. Xu, W.C. Yu, Y.T. Qian, Mater. Lett. 59 (2005) 3383–3388.
[17] Z.P. Peng, Y.S. Jiang, Y.H. Song, C. Wang, H.J. Zhang, Chem. Mater. 20 (2008) 3153–3162.
[18] M. Salavati-Niasari, A. Sobhani, F. Davar, J. Alloys Compd. 507 (2010) 77–83.
[19] R.M. El-Shazly, G.A.A. Al-Hazmi, Spectrochim. Acta A 71 (2009) 1885–1890.
[20] A.A. El-Asmy, Y.M. Shaibi, I.M. Shedaiwa, et al., J. Synth. React. Inorg. Met-Org. Chem. 18 (1988) 331–345.
[21] F. Zhang, S.S. Wong, Chem. Mater. 21 (2009) 454–4554.
[22] W. Li, D. Li, Z. Chen, H. Huang, M. Sun, Y. He, X. Fu, J. Phys. Chem. C 112 (2008) 14943–14947.